

Spin Liquid in the Multiple-Spin Exchange model on the Triangular lattice: ^3He on graphite

G. Misguich *, B. Bernu *, C. Lhuillier * and C. Waldtmann †
(August 7, 2018)

Using exact diagonalizations, we investigate the $T = 0$ phase diagram of the Multi-Spin Exchange (MSE) model on the triangular lattice: we find a transition separating a ferromagnetic phase from a non-magnetic gapped Spin Liquid phase. Systems far enough from the ferromagnetic transition have a metamagnetic behavior with magnetization plateaus at $m/m_{sat} = 0$ and $1/2$. The MSE has been proposed to describe solid ^3He films adsorbed onto graphite, thus we compute the MSE heat capacity for parameters in the low density range of the 2^{nd} layer and find a double-peak structure.

PACS numbers: 75.10.Jm; 75.50.Ee; 75.40.-s; 75.70.Ak

An increasing number of experiments on ^3He films have enforced the triangular lattice Multiple-Spin Exchange (MSE) picture of the solid second layer ([1,2] and references therein). Following Thouless [3,4], the magnetic properties of a 2-dimensional quantum crystal are described in spin space by the effective Hamiltonian:

$$H = - \sum_P (-1)^{\text{sign}(P)} J_P P \quad (1)$$

where P is any permutation operator of the spins of the lattice, and J_P equals one half of the (positive) tunneling frequency associated to the exchange process P . Whereas exchange of an even number of spins favors antiferromagnetism, odd processes are ferromagnetic. On the triangular lattice with spin $1/2$, two- and 3-body exchange reduce to an Heisenberg Hamiltonian with an effective $J_2^{\text{eff}} = J_2 - 2J_3$. In two-dimensional ^3He , because of stoichiometric hindrance, the 3-body process is much more efficient than the 2-body one, and the effective coupling constant is ferromagnetic. However, it was suspected since a long time that n -particle terms with $n > 3$ could not be ignored [5,1,6]. Very recently, a thorough analysis of susceptibility and heat capacity measurements enabled Roger and the Grenoble group [7] to establish the density dependence of the J 's and the importance of the 4-spin exchange J_4 in a large density range of the 2^{nd} layer: from the 2^{nd} layer solidification (AF solid) to the third layer promotion (F solid). This is in accordance with recent Path Integral Monte Carlo calculations which estimate $J_2^{\text{eff}}/J_4 \simeq -2 \pm 1$, $J_5/J_4 \simeq 1 \pm .5$ and $J_6/J_4 \simeq 1 \pm .5$ [8].

As first suggested by Roger in 1990 [9], 4-spin exchange strongly frustrates the system. Momoi, Kubo and Niki have recently studied the $J_2^{\text{eff}}-J_4$ model in the classical and semi-classical (spin-wave) limits and found numerous ordered phases: a ferromagnetic, a 4-sublattice ferrimagnetic phase, 3- and 4-sublattice AF phases and a chiral ordered phase [10,11]. Our $SU(2)$ Schwinger-Boson analysis of the $J_2^{\text{eff}}-J_4-J_5$ Hamiltonian also pointed to a rich phase diagram with Néel as well as helicoidal phases [12].

In the present work, exact diagonalizations results show that none of these $T=0$ Long Range Ordered (LRO) AF phases survive spin- $1/2$ quantum fluctuations. Instead, in the AF region, the system is a Quantum Spin Liquid (QSL) with short range spin-spin correlations, as suggested by Ishida *et al.* [13] and Kubo *et al.* [11].

We truncate Eq. (1) to the following simplest cyclic exchange patterns:

$$H = J_2^{\text{eff}} \sum_{\text{---}} P_2 + J_4 \sum_{\text{---}} (P_4 + P_4^{-1}) \quad (2)$$

$$- J_5 \sum_{\text{---}} (P_5 + P_5^{-1}) + J_6 \sum_{\text{---}} (P_6 + P_6^{-1})$$

The spin- $1/2$ permutation operators can be rewritten with usual spin operators (Pauli matrices): $P_{ij} = 2\mathbf{S}_i \cdot \mathbf{S}_j + 1/2$. $P_{1234} + h.c.$ and $P_{12345} + h.c.$ (resp. $P_{123456} + h.c.$) are polynomials of degree two (resp. three) in $\mathbf{S}_i \cdot \mathbf{S}_j$ [12,14]. The quantum phase diagram of this model is studied through the analysis of the finite size scaling of the low energy spectra of samples subjected to various boundary conditions (twisted or periodic with different shapes).

Ferro-antiferro transition.— We first look at the $T = 0$ ferro-antiferro transition line of Eq. (2). This line (see Fig. 1) is determined from about 50 spectra ($N = 19$) in the J_n space, with most points near the transition. Far all cases, the ground-state is either an $S = 0$ or an $S = N/2$ state. This excludes the possibility of a $vuud$ phase found in the classical calculations of Kubo *et al.* [11], which is ferrimagnetic and has a total spin $S = N/4$. The line where J_χ , the $1/T^2$ coefficient of the susceptibility, vanishes stands roughly parallel to the $T = 0$ F/AF line, inside the AF region. The density dependence of the J_n 's proposed by Roger *et al.* [7] for the second layer (see crosses in Figure 1) leads us to conclude that a $T=0$ transition to ferromagnetism occurs at $\rho_2 \simeq$

*Laboratoire de Physique Théorique des Liquides, Université P. et M. Curie, case 121, 4 Place Jussieu, 75252 Paris Cedex. UMR 7600 of CNRS.

†Institut für Theoretische Physik, Universität Hannover, D-30167 Hannover, Germany

$6.8 \pm 0.3nm^{-2}$ whereas $J\chi$ is zero at $\rho_2 \simeq 6.5nm^{-2}$ [7].

No Long Range Order.— The nature of the non magnetic or antiferromagnetic (AF) phase is a more challenging question. We first look for signatures of Néel Long Range Order (NLRO). NLRO is characterized on finite systems by very stringent spectral properties [15]: *i*) The symmetry breakings associated to the order parameter are embodied in a family of $\sim N^\alpha$ low lying levels collapsing to the ground-state in the thermodynamic limit (α is the number of magnetic sublattices). These levels with definite space and $SU(2)$ symmetries and dynamical properties should appear directly below the first magnon excitations. *ii*) The finite-size scalings of these levels are known. In particular, the ground-state energy per site $E(S = 0, N)/N$ has corrections scaling as $N^{-3/2}$, the $\Delta S = 1$ spin gap $E(S = 1, N) - E(S = 0, N)$ goes to zero as N^{-1} . None of these prescriptions is obeyed by the MSE spectra in the “S=0 ground-state” region displayed Fig. 1, whatever the twisted or shape boundary conditions may be. Thus, we exclude any commensurate or non-commensurate NLRO.

A $J_2^{eff} - J_4$ model.— We have analyzed in detail the $J_2^{eff} = -2, J_4 = 1$ model for nearly all possible systems from $N = 6$ to 30 and for $N = 36$. We noticed two different scaling behaviors: samples with N multiple of 4 or 6 have a low ground-state energy increasing with N whereas others samples have a high ground-state energy decreasing with N . The energies of both families merge for $N_0 \simeq 40$. Our interpretation is the following: N_0 is a crossover size above which the system is not anymore sensitive to boundary conditions and this is the signature of a finite length scale $\xi = \sqrt{N_0}$ in the ground-state wave function. This is supported by two facts: a fast decay of the spin-spin correlations with distance and a non-vanishing spin gap Δ in the thermodynamic limit. $\Delta S = 1$ gaps are plotted in Figure 2: the two families of samples (squares for N multiple of 4 or 6 and stars for others) have gaps of the order of 1 for $N > 24$. An estimation of the $N = \infty$ gap is possible using the strong correlation between E/N and Δ , the result is $\Delta \simeq 1.1 \pm 0.5$ (details will be given elsewhere).

These data point to a Quantum Spin Liquid state with a gap of the order of 1 for $J_2^{eff} = -2$ and $J_4 = 1$. This gap and the sensitivity to the geometrical shapes and boundary conditions of the small samples suggest a valence-bond picture of the ground-state and of the first triplet excitation.

Because of the strong frustration between the effective first neighbor ferromagnetic Heisenberg term (J_2^{eff}) and the 4-spin antiferromagnetic exchange, it is the triangular 6-spin plaquette which is the first system with a paramagnetic ($S = 0$) ground-state and a significant

gap¹. However the ground-state wave function is not a naive tensorial product of $S = 0$ independent triangle wave functions: such an approximation gives a very high ground-state energy (-2.8 to be compared to -4) and largely underestimates the gap ($.4$ to be compared to 1). This quasi independent triangle picture is thus deeply renormalized by resonances.

Analysis of the low lying levels in the $S = 0$ subspace leads to the same conclusion: the number of singlets below the first triplet level is very small (≤ 10 all degeneracy taken into account). As a comparison, this is very different from the Kagomé case where a continuum of singlets state is found in the magnetic gap [16,17]. Thus, this system seems a very example of a short range Resonating Valence Bond state with a clear cut gap in a translationally invariant 2-dimensional spin-1/2 model. Consequently, both the low temperature specific heat and spin susceptibility are thermally activated ($\chi(T) \sim e^{-\Delta/T}$, $C_V(T) \sim e^{-\Delta/T}$). However the gap decreases rapidly when approaching the AF/F transition and we are not yet able to decide if the gap vanishes at the transition to ferromagnetism or before. Indeed, experimental results of Ishida and collaborators seem to indicate either a very small gap or a quantum critical behavior [13].

2nd layer heat capacity.— We compute the MSE heat capacity for $J_2^{eff}/J_4 = -2$, $J_5/J_4 = 0.2$, $J_6/J_4 = 0.08$ with $N = 16, 20$ and 24 (Fig. 3) and find a clear low temperature peak. The entropy at $T/J_{C_v} = .5$ is $\simeq 0.4N \ln(2)$ and the low temperature peak is thus likely to remain in the thermodynamic limit. It also subsists for a relatively large range of competing J_n . Such a low temperature peak is characteristic of different highly frustrated systems [18,9]. The high temperature peak is located at a temperature of the order of J_{C_v} (J_{C_v} is the leading coefficient of the $1/T$ expansion of the specific heat: $C_v = 9/4(J_{C_v}/T)^2 + \mathcal{O}(1/T^3)$, its expression as a function of the J 's is given in [19]). The low temperature peak height and location do not only depend on J_{C_v} but also on the relative values of the coupling parameters. A better agreement between present results and experimental results [13] is expected by a fine tuning of the coupling parameters. Indeed, moving towards the boundary line between AF and F phases both decreases the gap and shifts the low temperature peak towards lower temperature.

Low energy degrees of freedom.— To understand the

¹ For $N = 24$ (resp. $N = 12$) one can compare the spectrum of the sample built with four (resp. two) 6-site triangles with the spectra computed from other shapes. The triangle-compatible shape gives the lowest energy and the largest gap (others have energies and gaps comparable with the frustrated family ones).

excitations responsible for this low energy peak we looked for possible common properties of low lying levels: it appears that most of these levels have a significant projection on the subspace engendered by spin-1 diamond tilings. This subspace \mathcal{E} is defined by the non-orthogonal family of wave functions:

$$|\Psi\rangle = \bigotimes_{d=1, \dots, \frac{N}{4}} |S_d = 1, S_d^z \in \{-1, 0, 1\}\rangle \quad (3)$$

where $|S_d = 1, S_d^z\rangle$ is the $S = 1, S^z = S_d^z$ state, symmetric with respect to the small diagonal of the d^{th} diamond. For $N = 16$ the projections of the exact low lying levels on \mathcal{E} range from 10% to 50% for nearly all the states involved in the peak (and drop under 1% for higher energy states). These numbers are very large compared with the expectation values of the projection of a random $S = 0$ or $S = 4$ wave function, which are, for the same lattice size, of the order of 1%. Since each tiling of the lattice gives $3^{\frac{N}{4}}$ independent states, the entropy associated with \mathcal{E} is at least $\ln(3^{\frac{N}{4}}) \simeq 0.4N \ln(3)$, in agreement with the low temperature peak entropy found in our samples.

These results lead to the following picture: At high temperature down to $T \simeq J_{C_v}$ the degrees of freedom are essentially random spin-1/2. For T less than J_{C_v} , the thermal wavelength increases and near neighbor spins behave coherently as weakly-ferromagnetic entities (pseudo spin-1). This explains the low temperature peak. At $T \simeq \Delta$ (spin gap), the 4-spin exchange coupling creates larger clusters and the system organizes itself as a QSL.

Magnetization.— Now we apply a magnetic field and look for the spin S of ground-state ($T=0$ magnetization). The large gap between the sectors of total spins $S = S_{max}/2$ and $S = S_{max}/2 + 1$ indicates that exciting one diamond to its $S = 2$ state costs a large energy. This feature gives rise to a low temperature plateau² at magnetization $m = 1/2$ (Fig. 3) which has also been found in the classical variational picture by Kubo *et al.* [11]. For the same coupling parameters as Fig. 3, the figure 4 shows two metamagnetic transitions at H_{C1} and H_{C2} and the magnetization is completely quantized³: $m = 0, 1/2$ or 1 . Thanks to the large gaps ($S = 0 \rightarrow 1$ and $S = N/4 \rightarrow N/4 + 1$) these plateaus survive thermal excitations. Close to the ferromagnetic transition (upper

² Related phenomena have already been encountered in the Heisenberg model with Ising anisotropy [20], in the MSE model on the square lattice [21], on Heisenberg ladders or chains [22,23]. An $m = 0$ plateau has been observed in the spin-ladder compound $Cu_2(C_5H_{12}N_2)_2Cl_4$ [24,25].

³ This, as well as the symmetries and degeneracies of the low lying levels of the spectra, will be discussed elsewhere in relation with possible extension of the Lieb-Schultz-Mattis theorem to 2-dimensional magnets [26,27].

black triangle of Fig. 1) both gaps decrease and the overall shape of the energy versus magnetization anticipates a transition to a phase where the magnetization curve is strongly non linear and reminiscent of the metamagnetic transitions (see [21] about metamagnetism in 3D solid ^3He).

In this letter we have shown that the spin-1/2 MSE model, in the range of parameters relevant for the description of ^3He on graphite, exhibits a transition from an antiferromagnetic phase at low density to a ferromagnetic one at high density. The AF phase has no Néel Long Range Order and is a Quantum Spin Liquid phase. In this phase the specific heat has two peaks. The lowest one testifies the building of a QSL out of short range pseudo spin-1. This picture is consistent with magnetization and heat capacity measurements. The microscopic arrangement of the spins may also show up as plateaus in the magnetization and $T = 0$ metamagnetic transitions between zero, half polarized and fully polarized phases.

Acknowledgments: We have benefited from very interesting discussions with C. Bäuerle, H. Fukuyama, H. Godfrin, K. Kubo, M. Roger and J. Saunders. Computations were performed on CRAY C94,C98 and T3E-256 at the Institut de Développement des Recherches en Informatique Scientifique of C.N.R.S. under contracts 960076/964091 and on CRAY T3E-512 of the Zentralinstitut für Angewandte Mathematik, Forschungszentrum Jülich.

-
- [1] H. Godfrin and R. E. Rapp, *Adv. Phys.* **44**, 113 (1995).
 - [2] M. Siqueira, J. Nyeki, B. Cowan, and J. Saunders, *Phys. Rev. Lett.* **78**, 2600 (1997).
 - [3] D.J. Thouless, *Proc. Phys. Soc.* **86**, 893 (1965).
 - [4] M. Roger, J.H. Hetherington and J.M. Delrieu, *Rev. Mod. Phys.* **55**, 1-63 (1983)
 - [5] D.S. Greywall, *Phys. Rev. B* **41**, 1842 (1990).
 - [6] M. Siqueira, J. Nyeki, B. Cowan, and J. Saunders, *Phys. Rev. Lett.* **76**, 1884 (1996).
 - [7] M. Roger, C. Bäuerle, Yu. M. Bunkov, A.-S. Chen and H. Godfrin, *Phys. Rev. Lett.* **80**, 1308 (1998).
 - [8] B. Bernu and D.M. Ceperley (unpublished).
 - [9] M. Roger, *Phys. Rev. Lett.* **64**, 297 (1990).
 - [10] T. Momoi, K. Kubo, and K. Niki, *Phys. Rev. Lett.* **79**, 2081 (1997).
 - [11] K. Kubo and T. Momoi, *Z. Phys. B. Condensed Matter* **103**, 485 (1997).
 - [12] G. Misguich, B. Bernu, and C. Lhuillier, *J. of Low Temp. Phys.* **110**, 327 (1998).
 - [13] K. Ishida, M. Morishita, K. Yawata, and H. Fukuyama, *Phys. Rev. Lett.* **79**, 3451 (1997).
 - [14] H. Godfrin and D. D. Osheroff, *Phys. Rev. B* **38**, 4492 (1988).
 - [15] B. Bernu, C. Lhuillier, and L. Pierre, *Phys. Rev. Lett.*

- 69, 2590 (1992). B. Bernu, P. Lecheminant, C. Lhuillier, and L. Pierre, Phys. Rev. B **50**, 10048 (1994).
- [16] P. Lecheminant, B. Bernu, C. Lhuillier, L. Pierre, and P. Sindzingre, Phys. Rev. B **56**, 2521 (1997).
- [17] C. Waldtmann, H.U. Everts, B. Bernu, C. Lhuillier, P. Sindzingre, P. Lecheminant, and L. Pierre, to appear in the European Journal of Physics.
- [18] V. Elser, Phys. Rev. Lett. **62**, 2405 (1989).
- [19] M. Roger, Phys. Rev. B **56**, R2928 (1997).
- [20] H. Nishimori and S. Miyashita, J. Phys. Soc. Jpn. **55**, 4448 (1986).
- [21] M. Roger and J.H. Hetherington, Phys. Rev. B **41**, 1 (1990).
- [22] D. C. Cabra, A. Honecker, and P. Pujol, Phys. Rev. Lett. **79**, 5126 (1997).
- [23] K. Totsuka, Phys. Rev. B **57**, 3454 (1998).
- [24] G. Chaboussant, P. A. Crowell, L. P. Levy, O. Piovesana, A. Madouri, and D. Maillly, Phys. Rev. B **55**, 3046 (1997).
- [25] C. A. Hayward, D. Poilblanc, and L. P. Levy, Phys. Rev. B **54**, R12649 (1996).
- [26] M. Oshikawa, M. Yamanaka, and I. Affleck, Phys. Rev. Lett. **78**, (1997)
- [27] I. Affleck, Phys. Rev. B **37**, 5186 (1988)

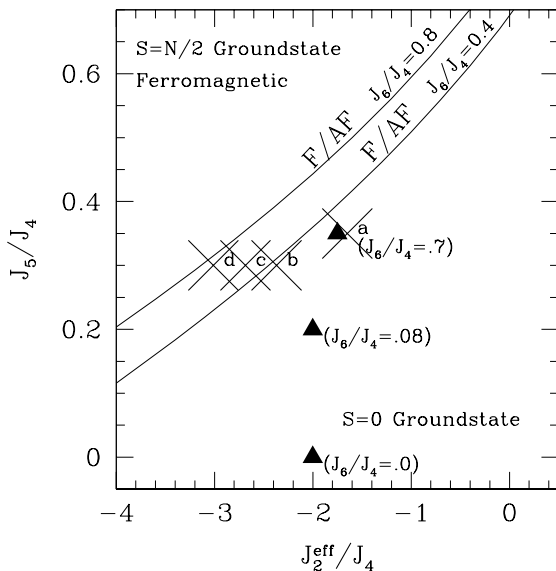


FIG. 1. Phase diagram for $J_2^{\text{eff}} < 0$. The solid line is the $T = 0$ transition line between ferromagnetic and antiferromagnetic phases. The crosses are Roger *et al*'s results [7] for four 2nd layer densities (nm^{-2}): $\rho_2^a = 6.5$ ($J_6/J_4 \simeq 0.7$), $\rho_2^b = 7.0$, $\rho_2^c = 7.65$ and $\rho_2^d = 7.8$. For b, c and d $J_6/J_4 \simeq 0.4$ (the size of the crosses may underestimate the uncertainties in the parameters). Two of the black triangles indicate the sets of coupling parameters corresponding to Fig. 2,3,4. The upper one is the point close to the frontier mentioned in the text.

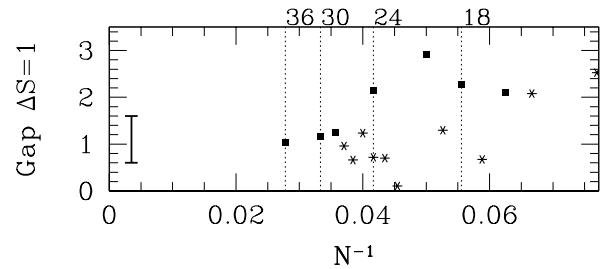


FIG. 2. Spin gap plotted as a function of $1/N$ for $J_2^{\text{eff}} = -2$, $J_4 = 1$. The vertical bar is the $N = \infty$ extrapolation made out of the $E/N \leftrightarrow \Delta$ correlation analysis.

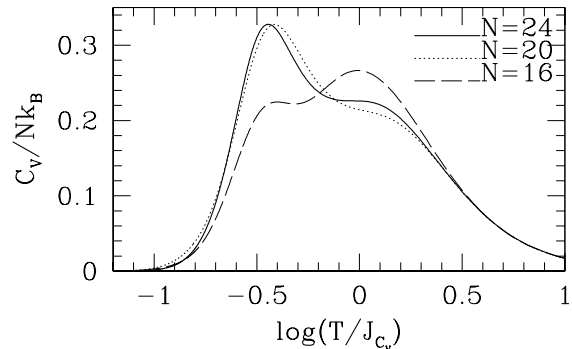


FIG. 3. Heat capacity versus temperature for three sizes. Coupling parameters are $J_2^{\text{eff}}/J_4 = -2$, $J_5/J_4 = 0.2$, $J_6/J_4 = 0.08$. For these values $J_{C_v} = 0.93J_4$ and the $N = \infty$ spin gap is of the order of $J_4/2$. Due to finite-size effects, on $N = 20$ and 24 the high temperature peak ($T \simeq J_{C_v}$) only shows up as a shoulder.

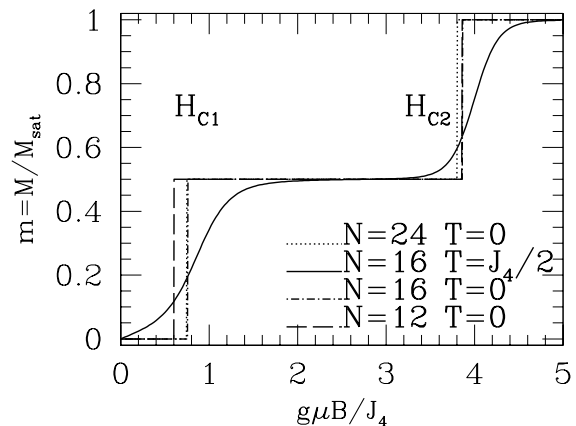


FIG. 4. Magnetization versus magnetic field B . Exchange parameters are those of Fig. 3. Since in ^3He , $J_4 \simeq 2mK$ and $g\mu = 1.5mK.T^{-1}$, H_{C1} is in the Tesla range.